Designing Ferromagnetic Soft Robots (FerroSoRo) with Level-Set-Based Multiphysics Topology Optimization

Jiawei Tian[1], Xuanhe Zhao[2], Xianfeng David Gu[3,4], and Shikui Chen[1*]

***Abstract*— Soft active materials can generate flexible locomotion and change configurations through large deformations when subjected to an external environmental stimulus. They can be engineered to design 'soft machines' such as soft robots, compliant actuators, flexible electronics, or bionic medical devices. By embedding ferromagnetic particles into soft elastomer matrix, the ferromagnetic soft matter can generate flexible movement and shift morphology in response to the external magnetic field. By taking advantage of this physical property, soft active structures undergoing desired motions can be generated by tailoring the layouts of the ferromagnetic soft elastomers. Structural topology optimization has emerged as an attractive tool to achieve innovative structures by optimizing the material layout within a design domain, and it can be utilized to architect ferromagnetic soft active structures. In this paper, the level-set-based topology optimization method is employed to design ferromagnetic soft robots (FerroSoRo). The objective function comprises a sub-objective function for the kinematics requirement and a sub-objective function for minimum compliance. Shape sensitivity analysis is derived using the material time derivative and adjoint variable method. Three examples, including a gripper, an actuator, and a flytrap structure, are studied to demonstrate the effectiveness of the proposed framework.**

I. INTRODUCTION

In response to an external environmental stimulus, soft active materials (SAM) can be programmed to generate adaptive and flexible movements through shape shifting, ranging from simple bending, folding, and torsion to complex transformations. In view of this, they have received increasingly significant attention in a wide range of tantalizing engineering applications such as soft robotics [1], [2], compliant electronics [3], [4] and bionic medical devices [5], [6] in recent years (Fig. 1). Differing from rigid-body machinery, where motions are generated by the change in the relative positions of rigid components, those soft machines can generate flexible motions and change various shapes through large deformation of the soft material [7].

To date, varieties of external fields, including magnetic field [13], electric field [14], acoustic field [15] and optical field [16], have been employed to manipulate soft active materials. Among these manipulation strategies, magnetic

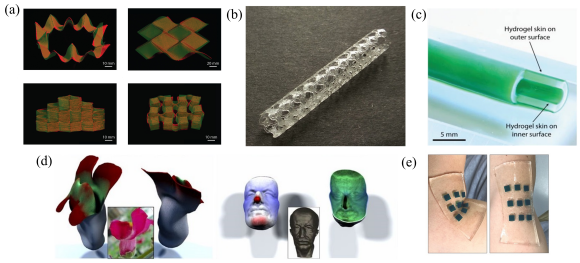

Fig. 1: Applications of soft materials. (a) Untethered fast-transforming magnetic soft materials [8]. (b) Image of 3D printed selfexpandable vascular stents [9]. (c) Hydrogel skins on inner and outer surface of medical tubing [10]. (d) Image of bionic flower petal and mask elastic bilayers [11]. (e) Conformal flexible electronics attached on human body [12].

stimulation holds numerous remarkable advantages, including remote and non-contact control, safe, biological-friendly, and promptly responsive to input signal [17]. Besides, the magnetic field can generate relatively higher forces and torques, which makes it possible to control both macroscopic scale objects as well as microcosmic particles [18], [19], [20].

Under the actuation of an external magnetic field, ferromagnetic soft elastomers can undergo large deformation by embedding ferromagnetic particles into the soft elastomer matrix. There exists a magnetic torque acting on the magnetized soft matter and forcing it twist to a new configuration, so the direction of the internal magnetization vector within the soft material is parallel to the direction of exterior magnetic flux density, as illustrated in Fig.2. By taking advantage of this physical property, many scientists have constructed this kind of magnetic soft materials to achieve desired movement and behaves. Most recently, Diller et al. [17] fabricated flexible magnetic planar structures by patterning hard magnetic particles in an ultraviolet lithography curable elastomer matrix. Kim et al. [8], [13] proposed a novel fabrication technique by applying an external magnetic field at the dispensing nozzle to reorient the hard magnetic particles during the printing process, with which the resultant designs can produce transitions from planar structures to complex 3D morphologies. Lum [21] investigated this subject and proposed a programming method that can automatically calculate the required magnetization and applied magnetic field for magnetic soft materials to achieve desired shapes. It is worth noting that all these existing works focused on the hard-magnetic soft materials, which have the ability to retain remnant magnetization even if the applied magnetic field is removed [8]. Indeed, it is the remnant magnetization

*Address all correspondence to S. Chen.
[1]Department of Mechanical Engineering, State University of New York, Stony Brook, NY, 11794, USA. (shikui.chen@stonybrook.edu; jiawei.tian@stonybrook.edu)
[2]Department of Mechanical Engineering, Massachusetts Institute of Technology, Cambridge, MA 02139, USA. (zhaox@mit.edu)
[3]Department of Computer Science, State University of New York, Stony Brook, NY, 11794, USA. (gu@cs.stonybrook.edu)
[4]Department of Applied Mathematics and Statistics, State University of New York, Stony Brook, NY, 11794, USA.

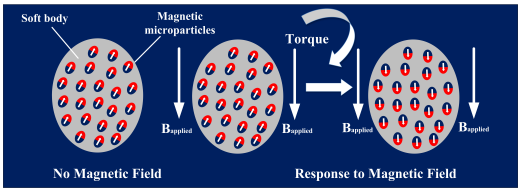

Fig. 2: Schematic representation of magnetic torque.

of the hard magnetic particles that enable the complex and convoluted shape shifting [17]. Although these magnetic soft robots are well fabricated and can achieve desired movements and functions, there are several limitations. First, all the shapes of soft elastomer matrix where the magnetic particles are patterned are 2D planar. There is no shape of matrix based on free-form surface, which is common in industrial applications [22], including flexible electronics [23], [24] and aircraft and aerospace structures [25], [26], [27]. In addition, the stiffness of these designed structures was not taken into consideration, which makes the design unattainable since soft robots need to sustain the reaction force when touching objects. More importantly, all these designs, to a large extent, relied on the designers' intuition or analogy to the existing designs, and a systematic design method for soft robots is yet absent.

Topology optimization (TO) can find an optimal layout of material in a design domain to attain desired performance of the structure, which has turned into an increasingly powerful and attractive tool in the engineering design field. TO was initially proposed to optimize light-weight load-carrying structures, but was later extended to diverse problems with multiphysics coupling characteristics, such as electromagnetics, thermomechanics, fluidics, acoustics [28], [29], [30]. Some investigations have been carried out to study designing soft robots using topology optimization. Most recently, Maute et al. designed a 4D printed heat-activating structure to produce large displacement using level set method and density-based method [31]. Chen et al. [32] designed a soft gripper actuated by cables in the form of a concentrated loading based on the level set method. Zhang et al. [33] proposed a framework to design multimaterial pneumatic soft fingers with maximal bending deflection through density-based topology optimization approach. In an earlier contribution, Wang and Chen et al. [34] proposed a level-set-based framework to design compliant mechanisms capable of transmitting motion from the input port to the output port. In these works, most of the designs were actuated by traditional contact force or pressure, and few studies investigated the non-contact actuation like magnetic stimulation over the volume of the geometry. Topology optimization of magnetic actuators has also been examined over the last decade [35], [36]; however, these investigations were mainly focused on magnetic energy instead of the kinematic performance.

In this study, the level-set-based topology optimization is employed to design ferromagnetic soft structures. It is worth noting that the structure is stimulated by a magnetic field which results in a magnetic body force (see Section.II in detail). It turns this optimization problem into a design-dependent problem since the magnetic load varies as the design evolves during the optimization process [37]. Moreover, the newly proposed extended level set method (X-LSM) [22] and conformal mapping theory [38], [39] are employed to carry out topology optimization of a FerroSoRo on a manifold.

The rest of the paper is organized as follows: Section.II introduces the ferromagnetic soft material (FSM) based actuation mechanism. Section.III presents details on the topology optimization for FerroSoRo, including the conventional level set method, X-LSM with conformal mapping theory, problem formulation, and shape sensitivity analysis, followed by three numerical examples given in Section.IV. Section.V concludes the paper and outlines future work.

II. ACTUATION MECHANISM OF FERROMAGNETIC SOFT MATERIAL

In this section, we briefly illustrate the actuation mechanism of ferromagnetic soft material (FSM) and recapitulate the basic governing equations of magnetism. For more details, the readers are referred to [40]. As discussed in Section.I, once placed in a uniform magnetic field, the ferromagnetic soft material will generate a torque $\boldsymbol{\tau}$, which can be calculated as

$$\boldsymbol{\tau} = \boldsymbol{M} \times \boldsymbol{B}. \tag{1}$$

In equation (1), $\boldsymbol{B}$ is the external magnetic flux density vector, and $\boldsymbol{M}$ is the magnetization of magnetic material.

In this paper, the torque caused by a uniform magnetic field is equivalently replaced with a magnetic body force to stimulate the ferromagnetic soft material.

Firstly, let's consider an external magnetic field generated by a pair of electromagnetic coils in air, as shown in Fig. 3. The symbols $\otimes$ and $\odot$ represent the directions the current flows in and out respectively. In a current-free space, the Maxwell equations governing a static magnetic field is defined as

$$\nabla \cdot \boldsymbol{B} = 0, \tag{2a}$$

$$curl(\boldsymbol{H}) = 0. \tag{2b}$$

In the above equations, $\boldsymbol{B}$ and $\boldsymbol{H}$ denote the magnetic flux density vector and the magnetic field intensity vector respectively, which are related by

$$\boldsymbol{B} = \mu_0 \left(\boldsymbol{H}+\boldsymbol{M}\right), \tag{3}$$

with μ_0 denoting the air permeability.

When a ferromagnetic soft material is placed in a magnetic filed, as shown in Fig.3, it will deform under the magnetic force caused by the applied magnetic field. The magnetic force $\boldsymbol{F}_m$ is calculated as [18], [21]

$$\boldsymbol{F}_m = \left(\boldsymbol{M} \cdot \nabla\right) \boldsymbol{B} = \mu_0 \left(\boldsymbol{M} \cdot \nabla\right) \boldsymbol{H}. \tag{4}$$

Rewriting the magnetic force with index notation results in the following scalar-valued function of the magnetic force:

$$F_{mi} = \mu_0 \left(M_x \frac{\partial H_i}{\partial x} + M_y \frac{\partial H_i}{\partial y} + M_z \frac{\partial H_i}{\partial z} \right), \tag{5}$$

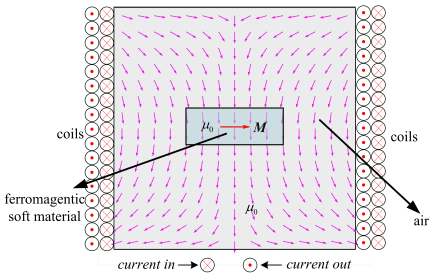

Fig. 3: Schematic representation of a ferromagnetic soft material placed in a magnetic filed.

where H_i is the component of magnetic field intensity in the ith direction; M_x, M_y and M_z are the components of magnetization in x, y, and z direction respectively.

From Eq. (3) and Eq. (4), it is noted that the magnetic field and the mechanics field are coupled bilaterally. Specifically, the emergence of the ferromagnetic soft material will perturb the external magnetic field, which in turn influences the applied force on the ferromagnetic soft material. To simplify the problem, we assume that the magnetic permeability of elastic continuum is the same as that of the ambient media (air), and the existence of ferromagnetic soft structure does not significantly alter the strong external magnetic field[8], [13]. Correspondingly, a mutual-coupling model is transformed into a one-way coupling model.

III. Topology Optimization of FerroSoRos

A. Conventional Level-Set-Based Topology Optimization

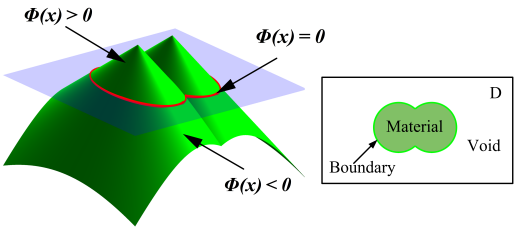

Fig. 4: A schematic of level set representation.

Conventionally, the level set function Φ is a Lipschitz continuous real-valued function defined in $\mathbb{R}^2$ or $\mathbb{R}^3$ [41]. The boundary of the design $\partial\Omega$ is implicitly represented as the zero level set of the function Φ, as illustrated in Fig. 4. According to the sign of the level set function, the design domain can be divided into three parts, denoting the material, the interface and the void respectively. The properties of the level set function can be formulated as equation (6):

$$\begin{cases} \Phi(x,t) > 0, & x \in \Omega, & \text{material} \\ \Phi(x,t) = 0, & x \in \bar{\Omega}, & \text{boundary} \\ \Phi(x,t) < 0, & x \in D/\Omega, & \text{void} \end{cases} \tag{6}$$

where D represents the design domain. The dynamics of the boundary evolution is governed by the Hamilton-Jacobi equation:

$$\frac{\partial \Phi(x,t)}{\partial t} - V_n |\nabla \Phi(x,t)| = 0, \tag{7}$$

where V_n is the normal velocity field.

B. Conformal Topology Optimization on Manifolds using Extended Level Set Method (X-LSM)

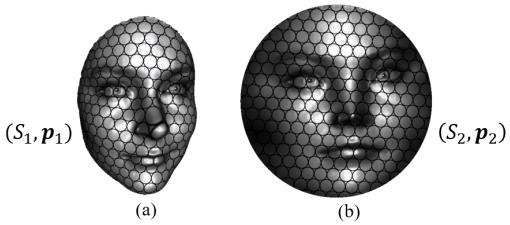

Fig. 5: Conformal mapping from the 3D surface to the 2D disk preserves infinitesimal circles. (a) infinitesimal circles on a 3D surface. (b) infinitesimal circles on a 2D disk.

Many bionic FerroSoRos exist in the form of curved thin-shell structures, or manifolds in a mathematical term. Conventional level set method only works in Euclidean space where the design domain is flat. How to implement level-set-based conformal topology optimization on a manifold is an important but challenging issue. The issue of conformal topology optimization has recently been addressed by Chen and Gu et al. [22], [42] by proposing an extended level set method (X-LSM) using the conformal mapping theory [38], [39].

The distinguishing feature of conformal mapping is that it conserves orientation and angles locally. As illustrated in Fig. 5, the shape of infinitesimal circles on the surface is well preserved on a 2D disk after mapping. The conformal mapping provides the point-to-point relation between the manifold and the 2D plane in the Euclidean space [43].

By employing the conformal mapping theory, we can conformally parameterize the manifold onto a 2D rectangular domain and evolve the design on the plane using the modified Hamilton-Jacobi equation as follows [22]:

$$\frac{\partial \Phi(x,t)}{\partial t} - e^{-\lambda} V_n |\nabla \Phi(x,t)| = 0, \tag{8}$$

where the λ is the *conformal factor* quantifying the scaling effect of the conformal mapping. In this way, X-LSM can transform a conformal topology optimization problem on Riemannian manifolds in 3D space to a 2D topology optimization problem in Euclidean space. It is worth noting that only with the conformal mapping we can attain such a concise Euclidean representation of the level set equation on the manifold, which otherwise would be extremely complex and computationally formidable.

C. Problem Formulation for FerroSoRo Design

The design problem for a FerroSoRo with desired kinematic performance and stiffness can be formulated as fol-

lows:

$$\begin{aligned} \textit{Minimize:} \quad J =& \omega_1 \left(\int_\Omega \boldsymbol{g} \cdot \boldsymbol{u} \mathrm{d}\Omega + \int_{\Gamma_N} \boldsymbol{f} \cdot \boldsymbol{u} \mathrm{d}s \right) \\ &+ \omega_2 \left(\int_\Omega k| \ \boldsymbol{u} - \boldsymbol{u}_0|^2 \mathrm{d}\Omega \right)^{\frac{1}{2}}, \qquad (9) \\ \textit{Subject to:} \quad & a(\boldsymbol{u}, \boldsymbol{v}) = l(\boldsymbol{v}), \quad \forall \boldsymbol{v} \in U \\ & V(\Omega) = V^*, \end{aligned}$$

where U stands for the space of kinematically admissible displacement fields [44]; $\boldsymbol{u}_0$ denotes the target displacement field; $\boldsymbol{u}$ denotes the actual displacement field; Ω indicates the material region in the design domain D. The boundary of the design is denoted by Γ, which comprises segments with Neumann boundary condition Γ_N, Dirichlet boundary condition Γ_D, and free boundary $\partial\Omega$. $\boldsymbol{g}$ and $\boldsymbol{f}$ denote the magnetic body force acting on the soft body and the traction force acting on the Neumann boundary Γ_N respectively. $V(\Omega)$ is the volume of the soft body, and V^* is the target volume. Localizing factor k is used to select the area of concern for kinematic performance. ω_1 and ω_2 are weighting factors for end compliance and kinematic target respectively. Here, $a(\boldsymbol{u}, \boldsymbol{v}) = l(\boldsymbol{v})$ is the weak form of governing equation. The energy form $a(\boldsymbol{u}, \boldsymbol{v})$ and the load form $l(\boldsymbol{v})$ as well as the volume $V(\Omega)$ are defined as

$$a(\boldsymbol{u}, \boldsymbol{v}) = \int_\Omega \epsilon_{ij}^T(\boldsymbol{u}) \mathbb{C}_{ijkl} \epsilon_{kl}(\boldsymbol{v}) \mathrm{d}\Omega, \qquad (10a)$$

$$l(\boldsymbol{v}) = \int_\Omega \boldsymbol{g} \cdot \boldsymbol{v} \mathrm{d}\Omega + \int_{\Gamma_N} \boldsymbol{f} \cdot \boldsymbol{v} \mathrm{d}s, \qquad (10b)$$

$$V(\Omega) = \int_D H(\Phi) \mathrm{d}\Omega, \qquad (10c)$$

where ϵ is the second-order linear strain tensor; $\mathbb{C}_{ijkl}$ is a fourth-order elastic stiffness tensor; $H(\Phi)$ represents the Heaviside function.

D. Shape Sensitivity Analysis

Topology optimization of FerroSoRo is a typical PDE-constrained optimization problem. To carry out the shape sensitivity analysis, Lagrangian method is employed to reformulate the PDE-constrained problem into an unconstrained optimization problem by coupling the objective function and governing equation as follows:

$$L(\boldsymbol{u}, \boldsymbol{v}) = J + \lambda \left(a(\boldsymbol{u}, \boldsymbol{v}) - l(\boldsymbol{v}) \right), \qquad (11)$$

where the λ is a Lagrange multiplier, and $\boldsymbol{v}$ is the adjoint displacement. Material time derivative is conducted to derive the shape sensitivity [41], [45], [44]:

$$\frac{DL(\boldsymbol{u}, \boldsymbol{v})}{Dt} = \frac{DJ}{Dt} + \frac{Da(\boldsymbol{u}, \boldsymbol{v})}{Dt} - \frac{Dl(\boldsymbol{v})}{Dt}. \qquad (12)$$

For conciseness, the derivative of the Lagrangian is directly presented as follows:

$$\begin{aligned} \frac{DL(\boldsymbol{u}, \boldsymbol{v})}{Dt} =& \omega_1 \int_\Gamma \boldsymbol{g} \cdot \boldsymbol{u} \boldsymbol{V}_n \mathrm{d}s + \frac{1}{2} \omega_2 D_0 \int_\Gamma k| \ \boldsymbol{u} - \boldsymbol{u}_0|^2 \boldsymbol{V}_n \mathrm{d}s \\ &+ \int_\Gamma \epsilon_{ij}(\boldsymbol{u}) \mathbb{C}_{ijkl} \epsilon_{kl}(\boldsymbol{v}) \boldsymbol{V}_n \mathrm{d}s - \int_\Gamma \boldsymbol{g} \cdot \boldsymbol{v} \boldsymbol{V}_n \mathrm{d}s, \end{aligned} \qquad (13)$$

where D_0 is a constant given by

$$D_0 = \left(\int_\Omega k| \ \boldsymbol{u} - \boldsymbol{u}_0|^2 \mathrm{d}\Omega \right)^{\frac{-1}{2}}. \qquad (14)$$

The adjoint displacement field $\boldsymbol{v}$ in Eq.13 can be obtained by solving the following equation with corresponding boundary condition.

$$\begin{aligned} &\int_\Omega \left(\omega_1 \boldsymbol{g} + \omega_2 D_0 k (\boldsymbol{u} - \boldsymbol{u}_0) \right) \cdot \boldsymbol{u}' \mathrm{d}\Omega \\ &+ \omega_1 \int_{\Gamma_N} \boldsymbol{f} \cdot \boldsymbol{u}' \mathrm{d}s + \int_\Omega \epsilon_{ij}^T(\boldsymbol{v}) \mathbb{C}_{ijkl} \epsilon_{kl}(\boldsymbol{u}') \mathrm{d}\Omega = 0. \end{aligned} \qquad (15)$$

With the steepest descent method, the normal design velocity with mean curvature κ and volume constraint can be constructed as

$$\begin{aligned} \boldsymbol{V}_n =& \boldsymbol{g} \cdot \boldsymbol{v} - \omega_1 \boldsymbol{g} \cdot \boldsymbol{u} - \frac{\omega_2 D_0}{2} k| \ \boldsymbol{u} - \boldsymbol{u}_0|^2 - \epsilon_{ij}(\boldsymbol{u}) \mathbb{C}_{ijkl} \epsilon_{kl}(\boldsymbol{v}) \\ &+ \lambda \left(V - V^* \right) + \iota \kappa, \end{aligned} \qquad (16)$$

where λ and ι are lagrangian multiplier for volume and perimeter constraint; κ is the curvature of the boundary.

IV. NUMERICAL EXAMPLES

A. Topology Optimization of a Magnetic Driven FerroSoRo Gripper

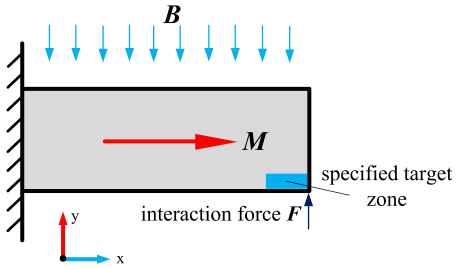

Fig. 6: The boundary conditions of the FerroSoRo gripper structure.

The first example is to achieve the optimal design of a 2-finger FerroSoRo gripper. Only one of the fingers is studied due to the symmetry. The dimension of the design domain is $2\,m \times 1\,m$. The properties of ferromagnetic soft material are set to be: Young's modulus $E = 1000\,Pa$, Poisson's ratio $\mu = 0.3$ and magnetization $M = 10^4\,A/m$. The dummy material with Young's modulus $E = 0.1\,Pa$ and magnetization $M = 1\,A/m$ are set for void. The target volume ratio is set to be 0.3. The boundary condition is shown in Fig.6, where the left side of design domain is fixed and a upward interaction force $\boldsymbol{F}$ with a magnitude of $1\,N$ is applied at the endpoint of the bottom edge to model the interaction between gripper and objects. The external magnetic field is $0.03\,T$, pointing downward, which is perpendicular to the direction of magnetization within ferromagnetic soft material. In this example, the localization factor k is chosen to be 1 on the blue zone (see Fig.6), and 0 elsewhere. The target displacement u_{y0} is set to be

$-0.2\ m$. The weighting factors for the end compliance and the kinematic target are set as $\omega_1 = 0.2$ and $\omega_2 = 0.8$ respectively.

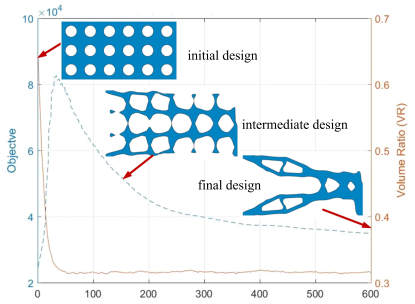

Fig. 7: Optimization history curve of the FerroSoRo gripper (upper finger).

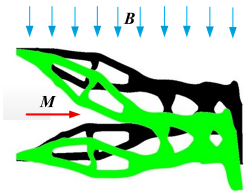

Fig. 8: Deformed configuration of the FerroSoRo gripper (upper finger).

The design evolution and iteration history curve of the optimization process are plotted in Fig.7. A downward bending configuration of final design under the actuation of magnetic field is shown in Fig.8, where the undeformed and deformed configurations are represented with shape in black and green respectively. Next, we extrude the 2D design into a 2.5D design to illustrate the process of grasping object in Fig.9, where two grippers with opposite magnetization direction are positioned as mirror symmetric distribution and mounted on a platform. With the stimulation of magnetic field, two grippers bend towards the center to grasp the object.

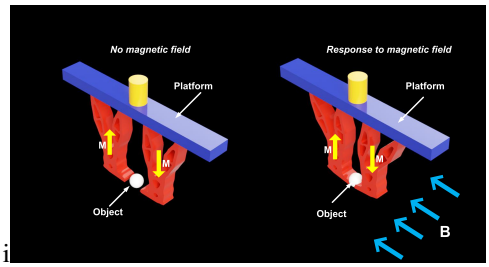

It i

Fig. 9: A schematic of grasping process.

B. Topology Optimization of a Magnetic Driven Actuator

The second example is to solve the optimal design of an actuator structure. The dimension of design domain is $2\,m \times 1\,m$. The properties of ferromagnetic soft elastomer and the dummy material are set as same as that in the first numerical example. The target volume ratio of actuator structure is 0.4.

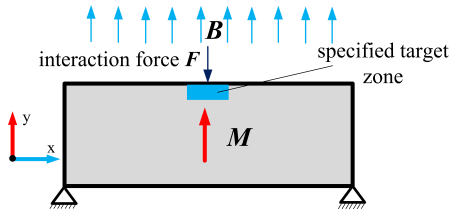

Fig. 10: Boundary condition of actuator structure.

The boundary condition is shown in Fig.10, where two end points of the bottom are fixed and downward interaction force $\boldsymbol{F}$ with magnitude of $1\,N$ is applied at the middle point of the top edge in order to model the reaction force given by object. The external magnetic field $\boldsymbol{B}$, rough $0.03T$ is applied with a direction same as the that of magnetization $\boldsymbol{M}$ so that the ferromagnetic soft structure has a tendency to expand. The blue area is selected as the area of concern for kinematic performance (see Fig.10) and the target displacement u_{y0} is set to be $0.2\ m$. The weighting factor ω_1 and ω_2 are still kept as 0.2 and 0.8.

Fig.11 is plotted to show the design evolution and iteration history curve of topology optimization. With the optimal design, an expanding and a contracting configuration can be achieved by changing the direction of applied magnetic field and the corresponding 2D and 2.5D deformed configurations are given in Fig.12.

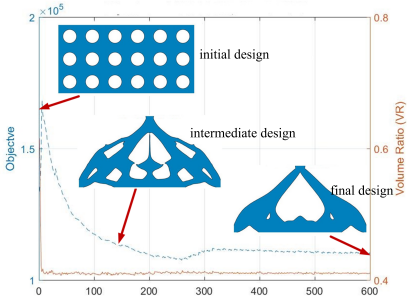

Fig. 11: Design evolution and iteration history curve of the actuator structure.

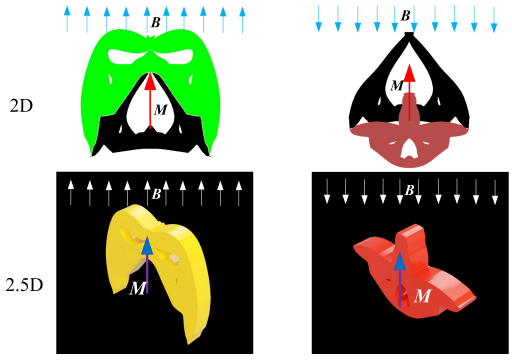

Fig. 12: Deformed configurations of the actuator structure.

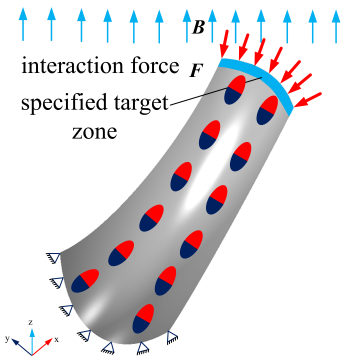

Fig. 13: Boundary condition of flytrap shell structure (only one finger).

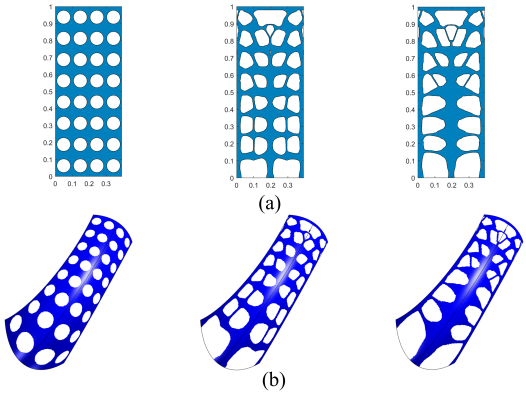

Fig. 14: Design evolution of the flytrap FerroSoRo structure. (a) Design evolution in 2D. (b) Design evolution on a petal surface.

C. Topology Optimization of a Magnetic Driven 5-Finger Flytrap Shell FerroSoRo

In this section, X-LSM is applied to design a flytrap shell structure, which mimics the flytrap plant in nature. The span of a single petal is approximately $2.5\ m \times 1.6\ m$ and the thickness is $0.05\ m$. The target volume ratio is 0.45. The material properties are assumed with a Young's modulus $E = 0.1\,MPa$, Poisson's ratio $\mu = 0.3$, and magnetization $M = 5 \times 10^4\,A/m$ with the direction of the positive axis x. To avoid singularity, a dummy material with Young's modulus $E = 10\,Pa$ and magnetization $M = 5\,A/m$ are set for void. The boundary condition for petal shell is shown in Fig.13, where the bottom edge is fixed and a interaction force $\boldsymbol{F} = (1, 0, -1)\ N$ is applied on the top edge. The blue area is chosen as the area of concern for kinematic performance and the target displacement are set as u_{x0}=$-0.5\ m$ and u_{z0}=$0.25\ m$, respectively. In addition, the weighting factor ω_1 and ω_2 are still kept as 0.2 and 0.8.

The elastic shell equilibrium equation is solved in 3D. In the optimization process, the petal surface is meshed with 63422 triangular elements before conformally mapped onto a $0.3923\ m \times 1\ m$ 2D rectangular domain where the level set function is defined and discretized with a 197×501 grid. During the implementation, the top layer of the petal is retained by setting design velocity is zero. The 2D design

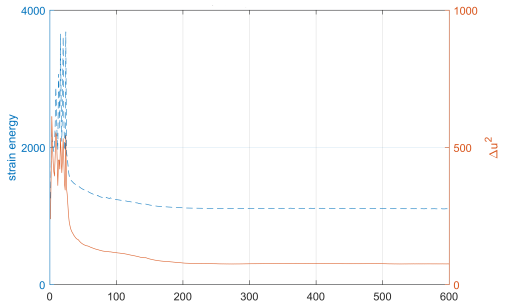

Fig. 15: The optimization history of flytrap shell structure.

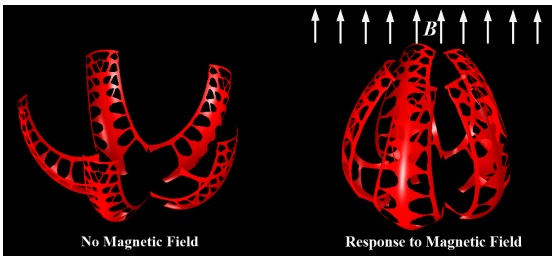

Fig. 16: Simulation of the grasping process of the flytrap FerroSoRo.

evolution and corresponding evolution on surfaces are shown in Fig.14. The optimization curves for compliance and target displacement are plotted in Fig.15. A flytrap structure can be achieved by making a circular pattern of this optimal petal shell structure. The simulation of the behavior of the design is presented in Fig.16.

V. CONCLUSIONS

In this paper, we have developed an effective level-set-based multiphysics topology optimization method for FerroSoRo design. Magnetic body force is adopted as the stimulation strategy to control ferromagnetic soft structures. At current stage, we simply the problem by assuming it is a linear elastic problem although we know that the soft material presents hyperelasticity. The ferromagnetic soft structures design problem is formulated as a balance of kinematic performance and minimum compliance. The three numerical examples have demonstrated the effectiveness of the proposed method for FerroSoRo design.

One of our future effort will concentrate on the design of multi-material nonlinear FerroSoRos. In virtue of additive manufacturing technology, the optimized FerroSoRos will be fabricated and corresponding experiments will be carried out to further validate their performances.

ACKNOWLEDGMENT

This work is supported by National Science Foundation (NSF) (CMMI-1462270,CMMI-1762287), the Ford University Research Program (URP) (Award No. 2017-9198R), and the start-up fund from the State University of New York at Stony Brook.

REFERENCES

[1] M. Wehner, R. L. Truby, D. J. Fitzgerald, B. Mosadegh, G. M. Whitesides, J. A. Lewis, and R. J. Wood, "An integrated design and fabrication strategy for entirely soft, autonomous robots," *Nature*, vol. 536, no. 7617, p. 451, 2016.

[2] S. Kim, C. Laschi, and B. Trimmer, "Soft robotics: a bioinspired evolution in robotics," *Trends in biotechnology*, vol. 31, no. 5, pp. 287–294, 2013.

[3] M. Zarek, M. Layani, I. Cooperstein, E. Sachyani, D. Cohn, and S. Magdassi, "3d printing of shape memory polymers for flexible electronic devices," *Advanced Materials*, vol. 28, no. 22, pp. 4449–4454, 2016.

[4] J. A. Fan, W.-H. Yeo, Y. Su, Y. Hattori, W. Lee, S.-Y. Jung, Y. Zhang, Z. Liu, H. Cheng, L. Falgout, *et al.*, "Fractal design concepts for stretchable electronics," *Nature communications*, vol. 5, p. 3266, 2014.

[5] X. Zhao, J. Kim, C. A. Cezar, N. Huebsch, K. Lee, K. Bouhadir, and D. J. Mooney, "Active scaffolds for on-demand drug and cell delivery," *Proceedings of the National Academy of Sciences*, vol. 108, no. 1, pp. 67–72, 2011.

[6] M. Cianchetti, C. Laschi, A. Menciassi, and P. Dario, "Biomedical applications of soft robotics," *Nature Reviews Materials*, p. 1, 2018.

[7] K. Asaka and H. Okuzaki, *Soft Actuators: Materials, Modeling, Applications, and Future Perspectives*. Springer, 2014.

[8] R. Zhao, Y. Kim, S. A. Chester, P. Sharma, and X. Zhao, "Mechanics of hard-magnetic soft materials," *Journal of the Mechanics and Physics of Solids*, vol. 124, pp. 244–263, 2019.

[9] H. Jia, S.-Y. Gu, and K. Chang, "3d printed self-expandable vascular stents from biodegradable shape memory polymer," *Advances in Polymer Technology*, vol. 37, no. 8, pp. 3222–3228, 2018.

[10] Y. Yu, H. Yuk, G. A. Parada, Y. Wu, X. Liu, C. S. Nabzdyk, K. Youcef-Toumi, J. Zang, and X. Zhao, "Multifunctional hydrogel skins on diverse polymers with arbitrary shapes," *Advanced Materials*, vol. 31, no. 7, p. 1807101, 2019.

[11] W. M. van Rees, E. Vouga, and L. Mahadevan, "Growth patterns for shape-shifting elastic bilayers," *Proceedings of the National Academy of Sciences*, vol. 114, no. 44, pp. 11 597–11 602, 2017.

[12] S. Lin, H. Yuk, T. Zhang, G. A. Parada, H. Koo, C. Yu, and X. Zhao, "Stretchable hydrogel electronics and devices," *Advanced Materials*, vol. 28, no. 22, pp. 4497–4505, 2016.

[13] Y. Kim, H. Yuk, R. Zhao, S. A. Chester, and X. Zhao, "Printing ferromagnetic domains for untethered fast-transforming soft materials," *Nature*, vol. 558, no. 7709, p. 274, 2018.

[14] W. Zhang, S. Ahmed, S. Masters, Z. Ounaies, and M. Frecker, "Finite element analysis of electroactive polymer and magnetoactive elastomer based actuation for origami-inspired folding," in *ASME 2016 Conference on Smart Materials, Adaptive Structures and Intelligent Systems*. American Society of Mechanical Engineers, 2016, pp. V001T01A001–V001T01A001.

[15] T. Brunet, A. Merlin, B. Mascaro, K. Zimny, J. Leng, O. Poncelet, C. Aristégui, and O. Mondain-Monval, "Soft 3d acoustic metamaterial with negative index," *Nature materials*, vol. 14, no. 4, p. 384, 2015.

[16] D. G. Grier, "A revolution in optical manipulation," *nature*, vol. 424, no. 6950, p. 810, 2003.

[17] T. Xu, J. Zhang, M. Salehizadeh, O. Onaizah, and E. Diller, "Millimeter-scale flexible robots with programmable three-dimensional magnetization and motions," *Science Robotics*, vol. 4, no. 29, p. eaav4494, 2019.

[18] R. M. Erb, J. J. Martin, R. Soheilian, C. Pan, and J. R. Barber, "Actuating soft matter with magnetic torque," *Advanced Functional Materials*, vol. 26, no. 22, pp. 3859–3880, 2016.

[19] A. Ranzoni, X. J. Janssen, M. Ovsyanko, L. J. van IJzendoorn, and M. W. Prins, "Magnetically controlled rotation and torque of uniaxial microactuators for lab-on-a-chip applications," *Lab on a Chip*, vol. 10, no. 2, pp. 179–188, 2010.

[20] R. M. Erb, N. J. Jenness, R. L. Clark, and B. B. Yellen, "Towards holonomic control of janus particles in optomagnetic traps," *Advanced materials*, vol. 21, no. 47, pp. 4825–4829, 2009.

[21] G. Z. Lum, Z. Ye, X. Dong, H. Marvi, O. Erin, W. Hu, and M. Sitti, "Shape-programmable magnetic soft matter," *Proceedings of the National Academy of Sciences*, vol. 113, no. 41, pp. E6007–E6015, 2016.

[22] Q. Ye, Y. Guo, S. Chen, N. Lei, and X. D. Gu, "Topology optimization of conformal structures on manifolds using extended level set methods (x-lsm) and conformal geometry theory," *Computer Methods in Applied Mechanics and Engineering*, vol. 344, pp. 164–185, 2019.

[23] H. C. Ko, M. P. Stoykovich, J. Song, V. Malyarchuk, W. M. Choi, C.-J. Yu, J. B. Geddes Iii, J. Xiao, S. Wang, Y. Huang, *et al.*, "A hemispherical electronic eye camera based on compressible silicon optoelectronics," *Nature*, vol. 454, no. 7205, p. 748, 2008.

[24] H. C. Ko, G. Shin, S. Wang, M. P. Stoykovich, J. W. Lee, D.-H. Kim, J. S. Ha, Y. Huang, K.-C. Hwang, and J. A. Rogers, "Curvilinear electronics formed using silicon membrane circuits and elastomeric transfer elements," *Small*, vol. 5, no. 23, pp. 2703–2709, 2009.

[25] J.-H. Zhu, W.-H. Zhang, and L. Xia, "Topology optimization in aircraft and aerospace structures design," *Archives of Computational Methods in Engineering*, vol. 23, no. 4, pp. 595–622, 2016.

[26] J.-w. Tian, K. Bu, J.-h. Song, G.-l. Tian, F. Qiu, D.-q. Zhao, Z.-l. Jin, and Y. Li, "Optimization of investment casting process parameters to reduce warpage of turbine blade platform in dd6 alloy," *China Foundry*, vol. 14, no. 6, pp. 469–477, 2017.

[27] R.-s. Jiang, D.-h. Zhang, K. Bu, W.-h. Wang, and J.-w. Tian, "A deformation compensation method for wax pattern die of turbine blade," *The International Journal of Advanced Manufacturing Technology*, vol. 88, no. 9-12, pp. 3195–3203, 2017.

[28] M. Bendsøe and O. Sigmund, "Theory, methods and applications," *Topology optimization. Springer, Berlin*, 2003.

[29] O. Sigmund and K. Maute, "Topology optimization approaches," *Structural and Multidisciplinary Optimization*, vol. 48, no. 6, pp. 1031–1055, 2013.

[30] N. P. van Dijk, K. Maute, M. Langelaar, and F. Van Keulen, "Level-set methods for structural topology optimization: a review," *Structural and Multidisciplinary Optimization*, vol. 48, no. 3, pp. 437–472, 2013.

[31] M. J. Geiss, N. Boddeti, O. Weeger, K. Maute, and M. L. Dunn, "Combined level-set-xfem-density topology optimization of four-dimensional printed structures undergoing large deformation," *Journal of Mechanical Design*, vol. 141, no. 5, p. 051405, 2019.

[32] F. Chen, W. Xu, H. Zhang, Y. Wang, J. Cao, M. Y. Wang, H. Ren, J. Zhu, and Y. Zhang, "Topology optimized design, fabrication, and characterization of a soft cable-driven gripper," *IEEE Robotics and Automation Letters*, vol. 3, no. 3, pp. 2463–2470, 2018.

[33] H. Zhang, A. S. Kumar, F. Chen, J. Y. Fuh, and M. Y. Wang, "Topology optimized multimaterial soft fingers for applications on grippers, rehabilitation, and artificial hands," *IEEE/ASME Transactions on Mechatronics*, vol. 24, no. 1, pp. 120–131, 2018.

[34] M. Y. Wang, S. Chen, X. Wang, and Y. Mei, "Design of multimaterial compliant mechanisms using level-set methods," *Journal of mechanical design*, vol. 127, no. 5, pp. 941–956, 2005.

[35] S.-i. Park and S. Min, "Design of magnetic actuator with nonlinear ferromagnetic materials using level-set based topology optimization," *IEEE Transactions on Magnetics*, vol. 46, no. 2, pp. 618–621, 2010.

[36] S.-i. Park, S. Min, S. Yamasaki, S. Nishiwaki, and J. Yoo, "Magnetic actuator design using level set based topology optimization," *IEEE Transactions on magnetics*, vol. 44, no. 11, pp. 4037–4040, 2008.

[37] J. D. Deaton and R. V. Grandhi, "A survey of structural and multidisciplinary continuum topology optimization: post 2000," *Structural and Multidisciplinary Optimization*, vol. 49, no. 1, pp. 1–38, 2014.

[38] X. Gu, Y. Wang, T. F. Chan, P. M. Thompson, and S.-T. Yau, "Genus zero surface conformal mapping and its application to brain surface mapping," *IEEE transactions on medical imaging*, vol. 23, no. 8, pp. 949–958, 2004.

[39] L. M. Lui, X. Gu, T. F. Chan, S.-T. Yau, *et al.*, "Variational method on riemann surfaces using conformal parameterization and its applications to image processing," *Methods and Applications of Analysis*, vol. 15, no. 4, pp. 513–538, 2008.

[40] P. Saxena, "On the general governing equations of electromagnetic acoustic transducers," *Archive of Mechanical Engineering*, vol. 60, no. 2, pp. 231–246, 2013.

[41] G. Allaire, F. Jouve, and A.-M. Toader, "Structural optimization using sensitivity analysis and a level-set method," *Journal of computational physics*, vol. 194, no. 1, pp. 363–393, 2004.

[42] Q. Ye, Y. Guo, S. Chen, X. D. Gu, and N. Lei, "Topology optimization of conformal structures using extended level set methods and conformal geometry theory," in *ASME 2018 International Design Engineering Technical Conferences and Computers and Information in Engineering Conference*. American Society of Mechanical Engineers Digital Collection, 2018.

[43] X. D. Gu and S.-T. Yau, *Computational conformal geometry*. International Press Somerville, MA, 2008.

[44] K. K. Choi and N.-H. Kim, *Structural sensitivity analysis and op-*

timization 1: linear systems. Springer Science & Business Media, 2006.

[45] M. Y. Wang, X. Wang, and D. Guo, "A level set method for structural topology optimization," *Computer methods in applied mechanics and engineering*, vol. 192, no. 1-2, pp. 227–246, 2003.